

Field-induced superconductivity mediated by odd-parity multipole fluctuation

Kosuke Nogaki^{1,*} and Youichi Yanase¹

¹*Department of Physics, Kyoto University, Kyoto 606-8502, Japan*

(Dated: December 13, 2023)

Field-induced superconductivity has long presented a counterintuitive phenomenon and a pivotal challenge in condensed matter physics. In this Letter, we introduce a mechanism for achieving field-induced superconductivity wherein the sublattice degree of freedom and the Coulomb interaction are tightly entwined. Our multipole-resolved analysis elucidates that lifting the fluctuation degeneracy results in an unconventional Cooper pairing channel, thereby realizing field-induced superconductivity. This research substantively augments the exploration of the latent potential of strongly correlated electron systems with sublattice degrees of freedom.

Introduction. — Superconductivity, which is typically suppressed by a magnetic field through both the Pauli and orbital-depairing effects [1], is paradoxically induced by the magnetic field in some systems. This counterintuitive phenomenon has garnered significant attention due to its implications for the unconventional origins of superconductivity. One of the well-known mechanisms of field-induced superconductivity is the Jaccarino-Peter effect [2, 3], which states that the external magnetic field compensates for the internal field produced by magnetic ions. Notably, the Chevrel phase superconductor $\text{Eu}_x\text{Sn}_{1-x}\text{Mo}_6\text{S}_8$ [4, 5] and the organic superconductors λ -(BETS)₂FeCl₄ [6, 7] and κ -(BETS)₂FeBr₄ [8] have been associated with the Jaccarino-Peter effect. In addition, the decrease of Kondo scattering [9, 10] and the reduction of the quasi-particle renormalization effect [11] have also been discussed as other possible mechanisms.

Field-induced superconductivity in uranium-based superconductors, as observed in compounds such as UGe₂ [12, 13], URhGe [14, 15], UCoGe [16, 17], and UTe₂ [18–21], has been established experimentally. This class of phenomena has predominantly been attributed to changes in effective interactions for Cooper pairing, specifically the amplification of ferromagnetic fluctuations. The application of a magnetic field brings these systems closer to a quantum critical point, which in turn enhances the strength of effective interactions responsible for the observed field-induced superconductivity [22–30].

Recently, the discovery of field-induced parity transition in CeRh₂As₂ has illuminated the role of sublattice degrees of freedom in heavy-fermion systems [31]. Subsequent intensive experimental and theoretical works have demonstrated that local inversion symmetry breaking can enable Cooper pairs to form odd-parity pairings in the high-magnetic-field phase [32–58]. Interestingly, similar sublattice structures in the unit cells are also inherent in the uranium compounds mentioned earlier. In addition, field-induced superconductivity has been reported in a locally-noncentrosymmetric cerium-based superconductor CeSb₂ [59, 60] and in magic-angle twisted trilayer graphene [61, 62]. Both uranium- and cerium-based superconductors, as well as moiré systems, may

have superconducting states driven by electron correlation effects. Given this, theoretical studies focusing on the strong correlation effect, sublattice degrees of freedom, and the magnetic field, are of significant interest. However, most of the previous theoretical studies have been based on the weak coupling theory. In particular, it should be noted that previous research has often assumed *degenerate* interactions in the sublattice degrees of freedom.

Effective Action. — In this Letter, we introduce a mechanism for field-induced superconductivity that originates from *degeneracy-lifted* pairing interactions in sublattice degrees of freedom. A theoretical basis for strongly correlated superconductors is the following effective action,

$$\begin{aligned} \mathcal{S}_{\text{eff}}[\bar{\psi}, \psi] &= \mathcal{S}_{\text{eff},0}[\bar{\psi}, \psi] + \mathcal{S}_{\text{eff,int}}[\bar{\psi}, \psi] \\ &= \sum_{\mathbf{k}} \bar{\psi}_{\mathbf{k},\alpha} (-i\omega_n \delta^{\alpha\beta} + \mathcal{H}_{\mathbf{k}}^{\alpha\beta} + \Sigma_{\mathbf{k}}^{\alpha\beta}) \psi_{\mathbf{k},\beta} \\ &+ \sum_{\mathbf{k},\mathbf{k}',q} \bar{\psi}_{\mathbf{k}+q,\alpha} \psi_{\mathbf{k},\beta} \Gamma_q^{\alpha\beta\gamma\delta} \bar{\psi}_{-\mathbf{k}',\delta} \psi_{-\mathbf{k}'+q,\gamma}, \quad (1) \end{aligned}$$

where abbreviated notation of $\mathbf{k} = (\mathbf{k}, i\omega_n)$, $q = (\mathbf{q}, i\nu_n)$, and $\alpha = (s, \sigma)$ are employed. Here, the momentum \mathbf{k} and the fermionic and bosonic Matsubara frequencies $\omega_n = (2n + 1)\pi T$, $\nu_n = 2n\pi T$ stand for the space-time dependence of the electron field $\psi_{\mathbf{k},\alpha}$ and the correlation functions. The index s and σ represent the spin and sublattice degrees of freedom, respectively. The $\mathcal{H}_{\mathbf{k}}^{\alpha\beta}$ is the single-particle Hamiltonian. We introduce the self-energy (Σ) and the vertex function (Γ); the former causes the renormalization of mass and damping of quasi-particles, while the latter drives the system toward superconductivity. These quantities obey the Ward-Takahashi identity: $\Sigma_{\mathbf{k}}^{\alpha\beta} = \sum_q \Gamma_q^{\alpha\gamma\beta\delta} G_{\mathbf{k}-q}^{\delta\gamma}$ [63, 64]. Here, $G_{\mathbf{k}}^{\alpha\beta} = -\langle \psi_{\mathbf{k},\alpha} \bar{\psi}_{\mathbf{k},\beta} \rangle$ describes the single-particle Green function. While the \mathbf{k} and \mathbf{k}' dependence of the vertex function are ignored for brevity, the extension of the following discussion to include such momentum dependence is straightforward [65, 66].

By virtue of diagrammatic techniques (e.g. the fluctuation exchange (FLEX) approximation [67–69] or Parquet

approximation [70, 71]), the above effective action can be derived from a bare action:

$$\begin{aligned} \mathcal{S}_{\text{bare}}[\bar{\psi}, \psi] &= \sum_{\mathbf{k}} \bar{\psi}_{\mathbf{k},\alpha} (-i\omega_n \delta^{\alpha\beta} + \mathcal{H}_{\mathbf{k}}^{\alpha\beta}) \psi_{\mathbf{k},\beta} \\ &+ \sum_{\mathbf{k},\mathbf{k}',q} \bar{\psi}_{\mathbf{k}+q,\alpha} \psi_{\mathbf{k},\beta} \Gamma_q^{0,\alpha\beta\gamma\delta} \bar{\psi}_{-\mathbf{k}',\delta} \psi_{-\mathbf{k}'+q,\gamma}. \end{aligned} \quad (2)$$

In this study, we focus on two-sublattice superconductors, including bilayer superconductors and two-fold nonsymmorphic crystalline superconductors. In the bare action, $\mathcal{H}_{\mathbf{k}}^{\alpha\beta}$ represents Hamiltonian of the two-sublattice system: $\mathcal{H}_{\mathbf{k}} = \varepsilon_{\mathbf{k}} s_0 \otimes \sigma_0 + \alpha \mathbf{g}_{\mathbf{k}} \cdot \mathbf{s} \otimes \sigma_z + t_{\perp} s_0 \otimes \sigma_x - \mu_B H s_z \otimes \sigma_0$. Here, $\varepsilon_{\mathbf{k}} = -2t(\cos k_x + \cos k_y) + 4t' \cos k_x \cos k_y - \mu$ and t_{\perp} represent intra- and inter-sublattice hopping term, respectively, and sublattice-dependent $\mathbf{g}_{\mathbf{k}} \cdot \mathbf{s}$ term represents staggered Rashba-type spin-orbit coupling which are originated from local inversion symmetry breaking [32, 72–83]. The \mathbf{g} -vector $\mathbf{g}_{\mathbf{k}} = [-\partial\varepsilon_{\mathbf{k}}/\partial k_y, \partial\varepsilon_{\mathbf{k}}/\partial k_x, 0]$ introduces the momentum-dependent spin polarization [84]. The H represents the Zeeman magnetic field parallel to the z -axis. The interaction term in the bare action is the Hubbard-type on-site Coulomb repulsion: $\mathcal{S}_{\text{bare,int}} = U \sum_{\sigma} \bar{\psi}_{i,\uparrow,\sigma} \psi_{i,\uparrow,\sigma} \bar{\psi}_{i,\downarrow,\sigma} \psi_{i,\downarrow,\sigma}$. The bare interaction tensor Γ^0 is obtained from the above Hubbard interaction [85].

The internal degrees of freedom of the two-sublattice model are classified by the augmented multipole operator \hat{Q} [86–88]: $\hat{Q}^{\mu\nu} = \sum_{\mathbf{k}} \bar{\psi}_{\mathbf{k}+q,\alpha} \mathcal{Q}_{\alpha\beta}^{\mu\nu} \psi_{\mathbf{k},\beta}$, where $\mathcal{Q}^{\mu\nu} = \bar{s}^{\mu} \otimes \bar{\sigma}^{\nu}$ satisfies the normalization condition $\text{tr}[\mathcal{Q}\mathcal{Q}^{\dagger}] = 1$ [85]. Here, $\bar{s}^{\mu} = s^{\mu}/\sqrt{2}$ ($\bar{\sigma}^{\mu} = \sigma^{\mu}/\sqrt{2}$) are the normalized Pauli and unit matrices. The interaction term $\mathcal{S}_{\text{eff,int}}$ can be expressed as the sum of the bi-linear interaction of the multipoles [89–93]:

$$\mathcal{S}_{\text{eff,int}}[\bar{\psi}, \psi] \approx \sum_{\mathcal{Q},q} \hat{Q}_q V_q^{\mathcal{Q}} \hat{Q}_{-q}, \quad (3)$$

where $V_q^{\mathcal{Q}} = \mathcal{Q}_{\alpha\beta} \Gamma_q^{\beta\alpha\gamma\delta} \mathcal{Q}_{\gamma\delta}$ describes the coupling constants of interaction between the augmented multipoles. For the sake of brevity, we here omit interactions between different multipoles.

From the multipole resolved interaction, a zero-momentum ($q = k - k' = 0$) Cooper pairing interaction can be obtained [65, 66]. The intra-sublattice even- and odd-parity multipole fluctuations, denoted by $\bar{\sigma}^0$ and $\bar{\sigma}^z$, result in the following Cooper pairing interactions [66]:

$$\begin{aligned} \mathcal{S}_{\sigma_0}[\bar{\psi}, \psi] &= \frac{1}{2} \sum_{\mathbf{k},\mathbf{k}'} V_{\mathbf{k}-\mathbf{k}'}^{\sigma_0} \{ \hat{\mathcal{P}}_{\mathbf{k}}^{0,\dagger} \hat{\mathcal{P}}_{\mathbf{k}'}^0 + \hat{\mathcal{P}}_{\mathbf{k}}^{z,\dagger} \hat{\mathcal{P}}_{\mathbf{k}'}^z \\ &+ \hat{\mathcal{P}}_{\mathbf{k}}^{x,\dagger} \hat{\mathcal{P}}_{\mathbf{k}'}^x + \hat{\mathcal{P}}_{\mathbf{k}}^{y,\dagger} \hat{\mathcal{P}}_{\mathbf{k}'}^y \}, \end{aligned} \quad (4)$$

$$\begin{aligned} \mathcal{S}_{\sigma_z}[\bar{\psi}, \psi] &= \frac{1}{2} \sum_{\mathbf{k},\mathbf{k}'} V_{\mathbf{k}-\mathbf{k}'}^{\sigma_z} \{ \hat{\mathcal{P}}_{\mathbf{k}}^{0,\dagger} \hat{\mathcal{P}}_{\mathbf{k}'}^0 + \hat{\mathcal{P}}_{\mathbf{k}}^{z,\dagger} \hat{\mathcal{P}}_{\mathbf{k}'}^z \\ &- \hat{\mathcal{P}}_{\mathbf{k}}^{x,\dagger} \hat{\mathcal{P}}_{\mathbf{k}'}^x - \hat{\mathcal{P}}_{\mathbf{k}}^{y,\dagger} \hat{\mathcal{P}}_{\mathbf{k}'}^y \}, \end{aligned} \quad (5)$$

where $\hat{\mathcal{P}}^{\mu} = \psi_{\alpha} \bar{\sigma}_{\alpha\beta}^{\mu} \psi_{\beta}$. In the degenerate case, where even- and odd-parity multipole interactions have the same coupling constant (i.e., $V_{\mathbf{k}-\mathbf{k}'} := V_{\mathbf{k}-\mathbf{k}'}^{\sigma_0} = V_{\mathbf{k}-\mathbf{k}'}^{\sigma_z}$), we obtain:

$$\mathcal{S}_{\text{degenerate}} = \sum_{\mathbf{k},\mathbf{k}'} V_{\mathbf{k}-\mathbf{k}'} \{ \hat{\mathcal{P}}_{\mathbf{k}}^{0,\dagger} \hat{\mathcal{P}}_{\mathbf{k}'}^0 + \hat{\mathcal{P}}_{\mathbf{k}}^{z,\dagger} \hat{\mathcal{P}}_{\mathbf{k}'}^z \}. \quad (6)$$

This is nothing but the frequently assumed pairing interaction for two-sublattice models [32, 73–78, 81, 94, 95]. When the degeneracy is lifted, the second-line terms in Eqs. (4) and (5) could result in unconventional inter-sublattice Cooper pairing channel. Field-induced superconductivity, a main result of this Letter, is attributed to such degeneracy-lifted interactions, which are ubiquitous in strongly correlated systems. The FLEX approximation extended to spin-orbit-coupled two-sublattice systems is employed to derive the effective action in this work [96–99]. Hereafter, we set $t' = 0.3$, $\mu_B = 1$, and $U = 3.9$ with a unit of energy $t = 1$ and determine the chemical potential so that the electron density per site n is 0.85. In the numerical study, we use 64×64 \mathbf{k} -meshes, and 16384, 8192, or 4096 Matsubara frequencies for $T = 0.004$, $0.004 < T < 0.01$, or $0.01 \leq T$, respectively [85].

Odd-parity multipole fluctuation. — For the later analysis, we discuss here the multipole susceptibilities without the self-energy, as detailed in the Supplemental materials [85]:

$$\chi^{\mathcal{Q}}(q) \approx \frac{\chi^{0,\mathcal{Q}}(q)}{1 - U^{\mathcal{Q}} \chi^{0,\mathcal{Q}}(q)}, \quad (7)$$

$$\chi^{0,\mathcal{Q}}(q) = \sum_{\mathbf{k}} \mathcal{Q}_{\eta\zeta}^{k-q,\mathbf{k}} \mathcal{Q}_{\zeta\eta}^{k,\mathbf{k}-q} L_{\zeta\eta}(\mathbf{k}, \mathbf{q}, i\nu_n), \quad (8)$$

where $\mathcal{Q}_{\zeta\eta}^{k,\mathbf{k}'} = \langle u_{\zeta,\mathbf{k}} | \mathcal{Q} | u_{\eta,\mathbf{k}'} \rangle$ and $L_{\zeta\eta}(\mathbf{k}, \mathbf{q}, i\nu_n) = -\frac{1}{N} \{ f(\varepsilon_{\eta,\mathbf{k}-\mathbf{q}}) - f(\varepsilon_{\zeta,\mathbf{k}}) \} / \{ i\nu_n + \varepsilon_{\eta,\mathbf{k}-\mathbf{q}} - \varepsilon_{\zeta,\mathbf{k}} \}$ represent the matrix element of the multipole operator \mathcal{Q} and the momentum-resolved Lindhard function between bands ζ and η , respectively. The eigenvector and eigenvalue of a band ζ of the Hamiltonian are denoted by $|u_{\zeta,\mathbf{k}}\rangle$ and $\varepsilon_{\zeta,\mathbf{k}}$. The symbol N represents the number of unit cells, and $f(\varepsilon)$ stands for the Fermi-Dirac distribution function. To activate the multipole \mathcal{Q} fluctuation, a sizable matrix element $\mathcal{Q}_{\eta\zeta}^{k-q,\mathbf{k}}$ and a positive interaction for the multipole, characterized by $U^{\mathcal{Q}} > 0$, are required. Thus, the electronic structure of the system inherently dictates the enhanced multipole fluctuation.

Herein, we demonstrate that a two-sublattice structure intrinsically favors odd-parity multipole fluctuations. Figure 1(a) illustrates the Fermi surfaces of our two-sublattice tight-binding model with two bands, labeled |1⟩ and |2⟩. Our system exhibits a type-II van Hove singularity resulting from the Rashba-type spin-orbit coupling [100–102]. Specifically, the type-II van Hove singularities are located around $\mathbf{k} = (\pm\delta, \pi)$, $(0, \pi \pm \delta)$,

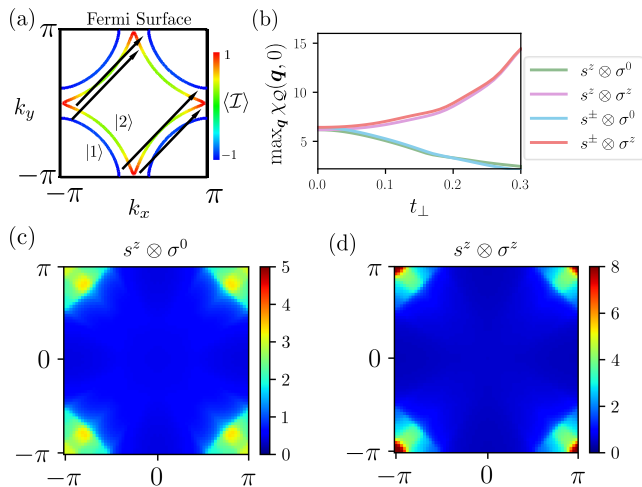


FIG. 1. (a) The Fermi surface of the two-sublattice tight-binding model with the model parameters: $\alpha = 0.2$, $t_{\perp} = 0.2$. The coloration on the Fermi surface signifies the expectation value of the inversion symmetry operator $\mathcal{I} = s_0 \otimes \sigma_z$. (b) The inter-sublattice hopping t_{\perp} dependence of static multipole fluctuations. The maximum of the even-parity (odd-parity) longitudinal (transverse) magnetic multipole susceptibilities are shown. Other multipole fluctuations are negligibly small. We assume $\alpha = 0.2$, $t_{\perp} = 0.2$ and $T = 0.01$. (c), (d) The momentum dependence of the even-parity and odd-parity longitudinal magnetic susceptibilities, respectively.

$(\pi, \pm\delta)$, and $(\pi \pm \delta, 0)$, away from the time-reversal invariant momentum that satisfies $\mathbf{K} = -\mathbf{K}$ modulo reciprocal lattice vectors. Figure 1(a) displays the expectation values of the inversion symmetry operator, $\mathcal{I} = s_0 \otimes \sigma_z$, on the Fermi surfaces. The bonding and anti-bonding orbitals defined as $|\text{BO}\rangle \equiv (1, 1)_{\sigma}^{\top}/\sqrt{2}$ and $|\text{ABO}\rangle \equiv (1, -1)_{\sigma}^{\top}/\sqrt{2}$ satisfy $\mathcal{I}|\text{BO}\rangle = |\text{BO}\rangle$ and $\mathcal{I}|\text{ABO}\rangle = -|\text{ABO}\rangle$. Considering that the expectation values of \mathcal{I} on the Fermi surfaces are close to ± 1 , we find that the wave functions around the type-II van Hove singularities are well approximated by either the bonding or anti-bonding orbitals.

In itinerant electron systems, multipole fluctuations emerge from the nesting of Fermi surfaces especially around van Hove singularities [103, 104]. Two potential nesting scenarios exist: one involves nesting within the same Fermi surface, either bonding to bonding or anti-bonding to anti-bonding. The other involves nesting between different Fermi surfaces, bonding to anti-bonding. The nesting vectors corresponding to each of these scenarios are illustrated in Fig. 1(a). Notably, while the nesting vectors connecting the same Fermi surface are not equivalent to each other, those connecting different Fermi surfaces are equivalent. As a result, in the two-sublattice model, nesting of different Fermi surfaces strongly enhances multipole fluctuations with operators having pronounced matrix elements between the Fermi

surfaces |1⟩ and |2⟩.

Employing the previously approximated wave functions, we can roughly evaluate the matrix element of the sublattice operator: $\langle 1|\sigma^0|1\rangle \approx \langle 1|\sigma^z|2\rangle \approx 1$ and $\langle 1|\sigma^0|2\rangle \approx \langle 1|\sigma^z|1\rangle \approx 0$. From this, it becomes evident that nesting within the same Fermi surface enhances even-parity multipole fluctuations while nesting between different Fermi surfaces results in odd-parity fluctuations. Combining these analyses, we conclude that the two-sublattice structure favors odd-parity multipole fluctuations, especially for large t_{\perp} and chemical potentials near the van Hove singularity.

The Hubbard-type Coulomb interaction can be expressed in the multipole basis as:

$$\mathcal{S}_{\text{int}} = -U \sum_{\nu=0,z} \hat{Q}_q^{0\nu} \hat{Q}_{-q}^{0\nu} + U \sum_{\substack{\mu=x,y,z \\ \nu=0,z}} \hat{Q}_q^{\mu\nu} \hat{Q}_{-q}^{\mu\nu}. \quad (9)$$

This expression for the multipole-resolved interaction implies that the Coulomb interaction equally enhances the even-parity and odd-parity magnetic multipoles. Figure 1(b) depicts the dependence of these multipole fluctuations on t_{\perp} , calculated using the FLEX approximation. As the inter-sublattice hopping parameter, t_{\perp} , increases, odd-parity fluctuations are notably enhanced while even-parity fluctuations are suppressed, consistent with the above discussions.

Figures 1(c)-(d) show the momentum dependence of multipole susceptibilities. The even-parity longitudinal magnetic fluctuation represented by the multipole operator $\hat{Q}^{z0} = \bar{s}^z \otimes \bar{\sigma}^0$ exhibits a double peak structure around $\mathbf{Q} \sim (\pi, \pi)$ and $(\pi - \delta, \pi - \delta)$ [Fig. 1(c)]. In contrast, the odd-parity longitudinal magnetic fluctuation given by the multipole operator $\hat{Q}^{zz} = \bar{s}^z \otimes \bar{\sigma}^z$ presents a single peak structure around $\mathbf{Q} \sim (\pi, \pi)$ [Fig. 1(d)]. These findings further substantiate the previous analysis of the nesting and wave functions of the Fermi surfaces, offering a more quantitative view. Note that the transverse magnetic fluctuations manifest a similar momentum dependence to the longitudinal ones.

It's worth noting that the Hubbard-type Coulomb interaction, as expressed by Eq. (9), has a degenerate form when viewed on a multipole basis. This suggests that all magnetic multipole interactions are equivalent at the mean-field level of analysis. However, the many-body effects lift the degeneracy through the intrinsic properties of the wave function of itinerant electrons, leading to the dominant odd-parity multipole fluctuation at low energies.

Superconductivity. — We here study superconductivity predominantly mediated by the odd-parity multipole fluctuations using the linearized Eliashberg equation [85]. Figure 2(a) depicts the magnetic field dependence of the eigenvalues of this equation. In the left figure for $t_{\perp} = 0.1$, the typical behavior of superconductivity under an external magnetic field is evident. All eigenvalues

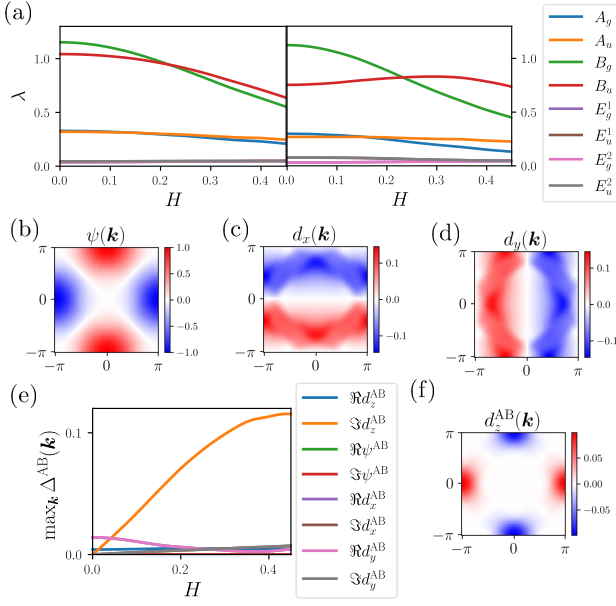


FIG. 2. (a) The magnetic field dependence of eigenvalues of the Éliashberg equation for each irreducible representation. We assume $\alpha = 0.2$ and $T = 0.01$. (Left) $t_{\perp} = 0.1$. (Right) $t_{\perp} = 0.2$. Superconducting instabilities are classified by the irreducible representation of the point group of the system, C_{4h} . The superscript of $E_{g/u}^{1,2}$ representations expresses the degeneracy lifted by time-reversal symmetry breaking due to the magnetic field. (b-d) The momentum dependence of intra-sublattice spin-singlet and spin-triplet gap functions, $\psi(\mathbf{k})$ and $\mathbf{d}(\mathbf{k})$, of the B_u representation for $H = 0.15$. Results for the B_g representation are almost the same as the figures. (e) The magnetic field dependence of the component-resolved weight of the inter-sublattice gap function. (f) The momentum dependence of the inter-sublattice spin-triplet gap function, $\Im d_z^{AB}(\mathbf{k})$.

across all irreducible representations are suppressed by the magnetic field. Notably, at $H = 0.22$, the eigenvalue curves of the B_g and B_u representations intersect. This intersection signals a phase transition from even-parity to odd-parity superconductivity, reminiscent of phenomena observed in CeRh_2As_2 [31, 44, 75]. In contrast, at $t_{\perp} = 0.2$ [right figure of Fig. 2(a)], the eigenvalue for the B_u representation increases upon magnetic field application, while that of B_g diminishes. Such behavior suggests the possible emergence of field-induced odd-parity superconductivity in the two-sublattice strongly correlated electron systems.

We delve into the mechanism behind this field-induced superconductivity. Initially, the intra-sublattice pair potential, given by $\Delta_{B_u}^{\text{intra}}(\mathbf{k}) = \psi(\mathbf{k})i s_y \otimes \sigma_z + \mathbf{d}(\mathbf{k}) \cdot \mathbf{s} i s_y \otimes \sigma_0$, is illustrated in Figs. 2(b)-(d). Influenced by the anti-ferromagnetic fluctuation, the spin-singlet component shows a $d_{x^2-y^2}$ -wave form. In addition, the spin-triplet components induced by the spin-orbit coupling display a p -wave momentum dependence. Interestingly,

these gap functions are relatively impervious to the external magnetic field [31, 44, 75]. Subsequently, the inter-sublattice pair potentials are analyzed. In Fig. 2(e), the component-resolved magnetic field dependence of inter-sublattice gap functions is shown. Evidently, the magnetic field induces a sizable spin-triplet and inter-sublattice anti-symmetric pair potential,

$$\Im d_z^{AB}(\mathbf{k}) s_z i s_y \otimes \sigma_y, \quad (10)$$

which is prohibited at the zero magnetic field by time-reversal symmetry. The momentum dependence of this pair potential is depicted in Fig. 2(f). Notably, Eq. (10) represents a σ_y -component in the sublattice degree of freedom. This implies that the pairing channel of \mathcal{P}_k^y in Eqs. (4) and (5), which arises from the lifting of degeneracy between even-parity and odd-parity multipole fluctuations, plays a pivotal role in the manifestation of field-induced superconductivity. In essence, the Cooper pairing inherent in Eq. (10) is fundamentally rooted in the multipole-mediated interactions, Eqs. (4) and (5), and the disruption of the time-reversal symmetry by the external magnetic field allows this pairing to emerge. As a result, the field-induced superconductivity occurs in the two-sublattice system through a cooperative interplay between the odd-parity multipole fluctuation and the magnetic field.

Further support for our interpretation of the mechanism behind field-induced superconductivity comes from considerations based on Feynman diagram analyses [85]. The gap function outlined in Eq. (10) plays a crucial role in facilitating the coupling between intra-sublattice gap functions through a second-order scattering process.

Phase diagram. — Figures 3(a)-(d) show the phase diagrams for $\alpha/t_{\perp} = 0, 0.5, 1,$ and 2 with $t_{\perp} = 0.2$. As expected, the odd-parity superconducting state exhibits field-induced behaviors in all cases. It is noteworthy that even in the case of $\alpha = 0$ (i.e., without spin-orbit coupling) the external magnetic field induces the odd-parity superconducting phase. Thus, the field-induced superconductivity does not require spin-orbit coupling. However, larger spin-orbit coupling renders the field-induced odd-parity superconducting phase more stable, as the transition temperature increases. Indeed, with spin-orbit coupling, the gap function in Eq. (10) incorporates intra-band components:

$$\Delta^{\pm}(\mathbf{k}) = \frac{d_z^{AB}(\mathbf{k})}{|\mathbf{g}(\mathbf{k})|^2 + t_{\perp}^2} \left\{ \mp \tilde{\mathbf{d}} \cdot \tilde{\mathbf{s}} + i \tilde{\psi}(\mathbf{k}) \tilde{s}_0 \right\} i \tilde{s}_y, \quad (11)$$

where $\tilde{\psi}(\mathbf{k}) = |\mathbf{g}(\mathbf{k})|^2$ and $\tilde{\mathbf{d}} = [g_y(\mathbf{k}), g_x(\mathbf{k}), 0]$. Consequently, the spin-orbit coupling significantly enhances the thermodynamic stability of the odd-parity superconducting phase.

The field-induced odd-parity superconducting state suffers from the Pauli depairing effect of Cooper pairs at extremely high fields, $H > 0.3$. Thus, the observed

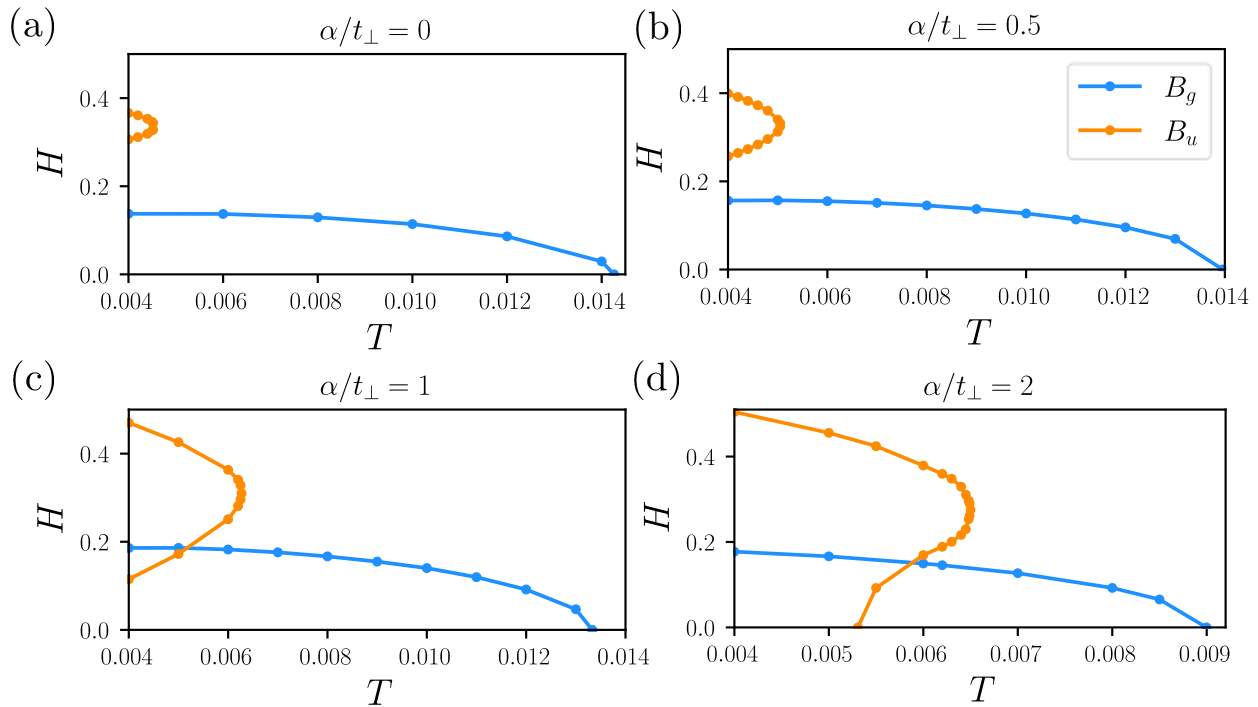


FIG. 3. (a)-(d) H - T phase diagrams of the two-sublattice Rashba-Hubbard model for $\alpha/t_{\perp} = 0, 0.5, 1, 2$. We show the superconducting transition lines of the even-parity B_g and odd-parity B_u states, on which eigenvalues of the Éliashberg equation become unity.

nonmonotonic behavior of the phase transition line of B_u state can result from the competition between the field-enhancement mechanism, associated with the inter-sublattice gap function, and the Pauli depairing effect.

Summary. — In summary, we have conducted a multipole-resolved analysis for unconventional superconductivity in strongly-correlated two-sublattice systems. The lifting of degeneracy between even- and odd-parity multipole fluctuations gives rise to the unconventional pairing channel. We demonstrated that the two-sublattice structure inherently favors multipole fluctuations with a predominating odd-parity nature, which induce sublattice-antisymmetric pairing only when the magnetic field is applied. Consequently, the field-induced superconductivity occurs. Notably, the obtained phase diagram reveals the field-reentrant odd-parity superconducting states.

Field-induced superconductivity within the bilayer model has also been proposed in previous studies [105–109]. In these theories, a magnetic field is posited to shift the energy levels of electronic states, thereby facilitating unconventional inter-band Cooper pairing. However, these models assume isotropic interaction within the layers, which distinctly sets them apart from the mechanism we present in this Letter. Note that the cornerstone of our proposal is the anisotropic effective interaction, a direct result of the degeneracy-lifted multipole fluctuation.

Finally, we would like to highlight a possible application of our theory. The electronic structure of magic-angle twisted trilayer graphene consists of a flat band from the moiré structure and a dispersive Dirac band in the absence of a displacement field [110–112]. The flat band potentially enhances the degenerated multipole fluctuation which is ensured by symmetry. For instance, fifteen-fold degenerate fluctuations protected by $SU(4)$ symmetry have been proposed in magic-angle twisted bilayer graphene [113]. The introduction of a displacement field leads to the hybridization of these bands, which could result in the lifting of the degeneracy in multipole fluctuations [62]. Application of an external magnetic field possibly induces unconventional Cooper pairing through the degeneracy-lifted multipole fluctuations as introduced in this Letter. This mechanism might explain the magnetic field-reentrant superconductivity observed in magic-angle twisted trilayer graphene [62]. Other potential candidates for application of this theory include uni-axially strained $CeRh_2As_2$ and pressurized $CeSb_2$ [60]. The pressure amplifies the inter-sublattice hopping and leads to the degeneracy-lifted multipole fluctuations. Comprehensive investigations into these phenomena are still highly anticipated.

The authors are grateful to A. Daido and S. Sumita for fruitful discussions. Some figures in this work were created by using FERMISURFER [114]. This work was sup-

ported by JSPS KAKENHI (Grants Nos. JP21K18145, 22H04933, JP22H01181, JP22KJ1716, JP23K17353).

* nogaki.kosuke.83v@st.kyoto-u.ac.jp

- [1] M. Tinkham, *Introduction to superconductivity*, 2nd ed. (Dover Publications Mineola, N.Y., Mineola, N.Y., 2004).
- [2] V. Jaccarino and M. Peter, Ultra-high-field superconductivity, *Phys. Rev. Lett.* **9**, 290 (1962).
- [3] O. H. Fischer, Properties of high-field superconductors containing localized magnetic moments., *Helv. Phys. Acta.* **45**, 331 (1972).
- [4] H. W. Meul, C. Rossel, M. Decroux, O. Fischer, G. Remenyi, and A. Briggs, Observation of magnetic-field-induced superconductivity, *Phys. Rev. Lett.* **53**, 497 (1984).
- [5] O. Fischer, H. W. Meul, M. G. Karkut, G. Remenyi, U. Welp, J. C. Piccoche, and K. Maki, Antivortex paramagnetism in the magnetic-field-induced superconducting state of $\text{Eu}_x\text{Sn}_{1-x}\text{Mo}_6\text{S}_8$, *Phys. Rev. Lett.* **55**, 2972 (1985).
- [6] S. Uji, H. Shinagawa, T. Terashima, T. Yakabe, Y. Terai, M. Tokumoto, A. Kobayashi, H. Tanaka, and H. Kobayashi, Magnetic-field-induced superconductivity in a two-dimensional organic conductor, *Nature* **410**, 908 (2001).
- [7] L. Balicas, J. S. Brooks, K. Storr, S. Uji, M. Tokumoto, H. Tanaka, H. Kobayashi, A. Kobayashi, V. Barzykin, and L. P. Gor'kov, Superconductivity in an organic insulator at very high magnetic fields, *Phys. Rev. Lett.* **87**, 067002 (2001).
- [8] T. Konoike, S. Uji, T. Terashima, M. Nishimura, S. Yasuzuka, K. Enomoto, H. Fujiwara, B. Zhang, and H. Kobayashi, Magnetic-field-induced superconductivity in the antiferromagnetic organic superconductor $\kappa\text{-(BETS)}_2\text{FeBr}_4$, *Phys. Rev. B* **70**, 094514 (2004).
- [9] A. N. Podmarkov and I. S. Sandalov, Recovery of superconductivity suppressed by magnetic impurities by use of a magnetic field, *Superconductor Science and Technology* **2**, 66 (1989).
- [10] A. N. Podmarkov and I. S. Sandalov, Possibility of magnetic-field-induced superconductivity in a metal with kondo impurities, *Journal of Experimental and Theoretical Physics* **68**, 1291 (1989).
- [11] M. Tachiki, B. D. Dunlap, G. W. Crabtree, S. Takahashi, and T. Koyama, Unusual temperature dependence of the upper critical field in superconducting heavy-fermion systems, *Phys. Rev. B* **34**, 7603 (1986).
- [12] S. S. Saxena, P. Agarwal, K. Ahilan, F. M. Grosche, R. K. W. Haselwimmer, M. J. Steiner, E. Pugh, I. R. Walker, S. R. Julian, P. Monthoux, G. G. Lonzarich, A. Huxley, I. Sheikin, D. Braithwaite, and J. Flouquet, Superconductivity on the border of itinerant-electron ferromagnetism in Uge_2 , *Nature* **406**, 587 (2000).
- [13] I. Sheikin, A. Huxley, D. Braithwaite, J. P. Brison, S. Watanabe, K. Miyake, and J. Flouquet, Anisotropy and pressure dependence of the upper critical field of the ferromagnetic superconductor Uge_2 , *Phys. Rev. B* **64**, 220503 (2001).
- [14] D. Aoki, A. Huxley, E. Ressouche, D. Braithwaite, J. Flouquet, J.-P. Brison, E. Lhotel, and C. Paulsen, Coexistence of superconductivity and ferromagnetism in Urhge , *Nature* **413**, 613 (2001).
- [15] F. Lévy, I. Sheikin, B. Grenier, and A. D. Huxley, Magnetic field-induced superconductivity in the ferromagnet Urhge , *Science* **309**, 1343 (2005), <https://www.science.org/doi/pdf/10.1126/science.1115498>.
- [16] N. T. Huy, A. Gasparini, D. E. de Nijs, Y. Huang, J. C. P. Klaasse, T. Gortenmulder, A. de Visser, A. Hamann, T. Görlach, and H. v. Löhneysen, Superconductivity on the border of weak itinerant ferromagnetism in Ucoge , *Phys. Rev. Lett.* **99**, 067006 (2007).
- [17] D. Aoki, T. D. Matsuda, V. Taufour, E. Hassinger, G. Knebel, and J. Flouquet, Extremely large and anisotropic upper critical field and the ferromagnetic instability in Ucoge , *Journal of the Physical Society of Japan* **78**, 113709 (2009).
- [18] S. Ran, C. Eckberg, Q.-P. Ding, Y. Furukawa, T. Metz, S. R. Saha, I.-L. Liu, M. Zic, H. Kim, J. Paglione, and N. P. Butch, Nearly ferromagnetic spin-triplet superconductivity, *Science* **365**, 684 (2019), <https://www.science.org/doi/pdf/10.1126/science.aav8645>.
- [19] D. Aoki, A. Nakamura, F. Honda, D. Li, Y. Homma, Y. Shimizu, Y. J. Sato, G. Knebel, J.-P. Brison, A. Pourret, D. Braithwaite, G. Lapertot, Q. Niu, M. Vališka, H. Harima, and J. Flouquet, Unconventional superconductivity in heavy fermion Ute_2 , *Journal of the Physical Society of Japan* **88**, 043702 (2019).
- [20] S. Ran, I.-L. Liu, Y. S. Eo, D. J. Campbell, P. M. Neves, W. T. Fuhrman, S. R. Saha, C. Eckberg, H. Kim, D. Graf, F. Balakirev, J. Singleton, J. Paglione, and N. P. Butch, Extreme magnetic field-boosted superconductivity, *Nature Physics* **15**, 1250 (2019).
- [21] G. Knebel, W. Knafo, A. Pourret, Q. Niu, M. Vališka, D. Braithwaite, G. Lapertot, M. Nardone, A. Zitouni, S. Mishra, I. Sheikin, G. Seyfarth, J.-P. Brison, D. Aoki, and J. Flouquet, Field-reentrant superconductivity close to a metamagnetic transition in the heavy-fermion superconductor Ute_2 , *Journal of the Physical Society of Japan* **88**, 063707 (2019), <https://doi.org/10.7566/JPSJ.88.063707>.
- [22] T. Hattori, Y. Ihara, Y. Nakai, K. Ishida, Y. Tada, S. Fujimoto, N. Kawakami, E. Osaki, K. Deguchi, N. K. Sato, and I. Satoh, Superconductivity induced by longitudinal ferromagnetic fluctuations in Ucoge , *Phys. Rev. Lett.* **108**, 066403 (2012).
- [23] K. Hattori and H. Tsunetsugu, p -wave superconductivity near a transverse saturation field, *Phys. Rev. B* **87**, 064501 (2013).
- [24] Y. Tada, S. Fujimoto, N. Kawakami, T. Hattori, Y. Ihara, K. Ishida, K. Deguchi, N. K. Sato, and I. Satoh, Spin-triplet superconductivity induced by longitudinal ferromagnetic fluctuations in Ucoge : Theoretical aspect, *Journal of Physics: Conference Series* **449**, 012029 (2013).
- [25] T. Hattori, K. Karube, K. Ishida, K. Deguchi, N. K. Sato, and T. Yamamura, Relationship between ferromagnetic criticality and the enhancement of superconductivity induced by transverse magnetic fields in Ucoge , *Journal of the Physical Society of Japan* **83**, 073708 (2014).
- [26] Y. Tokunaga, D. Aoki, H. Mayaffre, S. Krämer, M.-H. Julien, C. Berthier, M. Horvatić, H. Sakai, S. Kambe, and S. Araki, Reentrant superconductivity driven by

- quantum tricritical fluctuations in urhge: Evidence from ^{59}Co nmr in $\text{urh}_{0.9}\text{co}_{0.1}\text{Ge}$, *Phys. Rev. Lett.* **114**, 216401 (2015).
- [27] Y. Tokunaga, D. Aoki, H. Mayaffre, S. Krämer, M.-H. Julien, C. Berthier, M. Horvatić, H. Sakai, T. Hattori, S. Kambe, and S. Araki, Interplay between quantum fluctuations and reentrant superconductivity with a highly enhanced upper critical field in urhge, *Phys. Rev. B* **93**, 201112 (2016).
- [28] Y. Tada, S. Takayoshi, and S. Fujimoto, Magnetism and superconductivity in ferromagnetic heavy-fermion system ucoge under in-plane magnetic fields, *Phys. Rev. B* **93**, 174512 (2016).
- [29] B. Wu, G. Bastien, M. Taupin, C. Paulsen, L. Howald, D. Aoki, and J.-P. Brison, Pairing mechanism in the ferromagnetic superconductor ucoge, *Nature Communications* **8**, 14480 (2017).
- [30] A. Rosuel, C. Marcenat, G. Knebel, T. Klein, A. Pourret, N. Marquardt, Q. Niu, S. Rousseau, A. Demuer, G. Seyfarth, G. Lapertot, D. Aoki, D. Braithwaite, J. Flouquet, and J. P. Brison, Field-induced tuning of the pairing state in a superconductor, *Phys. Rev. X* **13**, 011022 (2023).
- [31] S. Khim, J. F. Landaeta, J. Banda, N. Bannor, M. Brando, P. M. R. Brydon, D. Hafner, R. Küchler, R. Cardoso-Gil, U. Stockert, A. P. Mackenzie, D. F. Agterberg, C. Geibel, and E. Hassinger, Field-induced transition within the superconducting state of $\text{cerh}_{\text{sub}i2\text{i}/\text{sub}i\text{as}}\text{sub}_{i2\text{i}/\text{sub}i}$, *Science* **373**, 1012 (2021), <https://www.science.org/doi/pdf/10.1126/science.abe7518>.
- [32] E. G. Schertenleib, M. H. Fischer, and M. Sigrist, Unusual $h-t$ phase diagram of Cerh_2as_2 : The role of staggered noncentrosymmetry, *Phys. Rev. Res.* **3**, 023179 (2021).
- [33] D. Möckli and A. Ramires, Two scenarios for superconductivity in cerh_2as_2 , *Phys. Rev. Res.* **3**, 023204 (2021).
- [34] A. Ptok, K. J. Kapcia, P. T. Jochym, J. Łażewski, A. M. Oleś, and P. Piekarczyk, Electronic and dynamical properties of cerh_2as_2 : Role of rh_2as_2 layers and expected orbital order, *Phys. Rev. B* **104**, L041109 (2021).
- [35] K. Nogaki, A. Daido, J. Ishizuka, and Y. Yanase, Topological crystalline superconductivity in locally noncentrosymmetric cerh_2as_2 , *Phys. Rev. Res.* **3**, L032071 (2021).
- [36] D. Möckli and A. Ramires, Superconductivity in disordered locally noncentrosymmetric materials: An application to cerh_2as_2 , *Phys. Rev. B* **104**, 134517 (2021).
- [37] S.-i. Kimura, J. Sichelschmidt, and S. Khim, Optical study of the electronic structure of locally noncentrosymmetric Cerh_2as_2 , *Phys. Rev. B* **104**, 245116 (2021).
- [38] S. Onishi, U. Stockert, S. Khim, J. Banda, M. Brando, and E. Hassinger, Low-temperature thermal conductivity of the two-phase superconductor cerh_2as_2 , *Frontiers in Electronic Materials* **2**, 10.3389/femat.2022.880579 (2022).
- [39] D. C. Cavanagh, T. Shishidou, M. Weinert, P. M. R. Brydon, and D. F. Agterberg, Nonsymmorphic symmetry and field-driven odd-parity pairing in Cerh_2as_2 , *Phys. Rev. B* **105**, L020505 (2022).
- [40] D. Hafner, P. Khanenko, E.-O. Eljaouhari, R. Küchler, J. Banda, N. Bannor, T. Lühmann, J. F. Landaeta, S. Mishra, I. Sheikin, E. Hassinger, S. Khim, C. Geibel, G. Zwicknagl, and M. Brando, Possible quadrupole density wave in the superconducting kondo lattice cerh_2as_2 , *Phys. Rev. X* **12**, 011023 (2022).
- [41] M. Kibune, S. Kitagawa, K. Kinjo, S. Ogata, M. Manago, T. Taniguchi, K. Ishida, M. Brando, E. Hassinger, H. Rosner, C. Geibel, and S. Khim, Observation of antiferromagnetic order as odd-parity multipoles inside the superconducting phase in cerh_2as_2 , *Phys. Rev. Lett.* **128**, 057002 (2022).
- [42] S. Kitagawa, M. Kibune, K. Kinjo, M. Manago, T. Taniguchi, K. Ishida, M. Brando, E. Hassinger, C. Geibel, and S. Khim, Two-dimensional xy-type magnetic properties of locally noncentrosymmetric superconductor cerh_2as_2 , *Journal of the Physical Society of Japan* **91**, 043702 (2022).
- [43] T. Hazra and P. Coleman, Triplet pairing mechanisms from hund's-kondo models: Applications to ute_2 and cerh_2as_2 , *Phys. Rev. Lett.* **130**, 136002 (2023).
- [44] K. Nogaki and Y. Yanase, Even-odd parity transition in strongly correlated locally noncentrosymmetric superconductors: Application to cerh_2as_2 , *Phys. Rev. B* **106**, L100504 (2022).
- [45] J. F. Landaeta, P. Khanenko, D. C. Cavanagh, C. Geibel, S. Khim, S. Mishra, I. Sheikin, P. M. R. Brydon, D. F. Agterberg, M. Brando, and E. Hassinger, Field-angle dependence reveals odd-parity superconductivity in cerh_2as_2 , *Phys. Rev. X* **12**, 031001 (2022).
- [46] K. Machida, Violation of pauli-clogston limit in the heavy-fermion superconductor cerh_2as_2 : Duality of itinerant and localized $4f$ electrons, *Phys. Rev. B* **106**, 184509 (2022).
- [47] H. Siddiquee, Z. Rehfuss, C. Broyles, and S. Ran, Pressure dependence of superconductivity in cerh_2as_2 , *Phys. Rev. B* **108**, L020504 (2023).
- [48] S. Mishra, Y. Liu, E. D. Bauer, F. Ronning, and S. M. Thomas, Anisotropic magnetotransport properties of the heavy-fermion superconductor cerh_2as_2 , *Phys. Rev. B* **106**, L140502 (2022).
- [49] C. Lee and S. B. Chung, Linear optical response from the odd parity bardasis-schrieffer mode in locally non-centrosymmetric superconductors (2022), [arXiv:2212.13722 \[cond-mat.supr-con\]](https://arxiv.org/abs/2212.13722).
- [50] K. Semeniuk, D. Hafner, P. Khanenko, T. Lühmann, J. Banda, J. F. Landaeta, C. Geibel, S. Khim, E. Hassinger, and M. Brando, Superconductivity versus quadrupole density wave in cerh_2as_2 (2023), [arXiv:2301.09151 \[cond-mat.supr-con\]](https://arxiv.org/abs/2301.09151).
- [51] S. Ogata, S. Kitagawa, K. Kinjo, K. Ishida, M. Brando, E. Hassinger, C. Geibel, and S. Khim, Parity transition of spin-singlet superconductivity using sublattice degrees of freedom, *Phys. Rev. Lett.* **130**, 166001 (2023).
- [52] N. A. Hackner and P. M. R. Brydon, Bardasis-schrieffer-like phase mode in a superconducting bilayer (2023), [arXiv:2306.16611 \[cond-mat.supr-con\]](https://arxiv.org/abs/2306.16611).
- [53] A. L. Szabó, M. H. Fischer, and M. Sigrist, Effects of nucleation at a first-order transition between two superconducting phases: Application to cerh_2as_2 (2023), [arXiv:2307.10374 \[cond-mat.supr-con\]](https://arxiv.org/abs/2307.10374).
- [54] D. S. Christovam, M. Ferreira-Carvalho, A. Marino, M. Sundermann, D. Takegami, A. Melendez-Sans, K. D. Tsuei, Z. Hu, S. Roessler, M. Valvidares, M. W. Haverkort, Y. Liu, E. D. Bauer, L. H. Tjeng, G. Zwicknagl, and A. Severing, Spectroscopic evidence of kondo-induced quasi-quartet in cerh_2as_2 (2023),

- arXiv:2308.10663 [cond-mat.str-el].
- [55] A. Szabo and A. Ramirez, Superconductivity-induced improper orders (2023), arXiv:2309.05664 [cond-mat.supr-con].
- [56] X. Chen, L. Wang, J. Ishizuka, K. Nogaki, Y. Cheng, F. Yang, R. Zhang, Z. Chen, F. Zhu, Y. Yanase, B. Lv, and Y. Huang, Coexistence of near-ef flat band and van hove singularity in a two-phase superconductor (2023), arXiv:2309.05895 [cond-mat.str-el].
- [57] Y. Wu, Y. Zhang, S. Ju, Y. Hu, G. Yang, H. Zheng, Y. Huang, Y. Zhang, H. Zhang, B. Song, N. C. Plumb, F. Steglich, M. Shi, G. Zwirgagl, C. Cao, H. Yuan, and Y. Liu, Quasi-two-dimensional fermi surface and heavy quasiparticles in cerh2as2 (2023), arXiv:2309.06732 [cond-mat.str-el].
- [58] J. Ishizuka, K. Nogaki, M. Sigrist, and Y. Yanase, Correlation-induced fermi surface evolution and topological crystalline superconductivity in cerh2as2 (2023), arXiv:2311.00324 [cond-mat.supr-con].
- [59] P. C. Canfield, J. D. Thompson, and Z. Fisk, Novel Ce magnetism in CeDipnictide and Di-Ce pnictide structures, *Journal of Applied Physics* **70**, 5992 (1991), https://pubs.aip.org/aip/jap/article-pdf/70/10/5992/8021380/5992_1_online.pdf.
- [60] O. P. Squire, S. A. Hodgson, J. Chen, V. Fedoseev, C. K. de Podesta, T. I. Weinberger, P. L. Alireza, and F. M. Grosche, Superconductivity beyond the conventional pauli limit in high-pressure cesb₂, *Phys. Rev. Lett.* **131**, 026001 (2023).
- [61] J. M. Park, Y. Cao, K. Watanabe, T. Taniguchi, and P. Jarillo-Herrero, Tunable strongly coupled superconductivity in magic-angle twisted trilayer graphene, *Nature* **590**, 249 (2021).
- [62] Y. Cao, J. M. Park, K. Watanabe, T. Taniguchi, and P. Jarillo-Herrero, Pauli-limit violation and re-entrant superconductivity in moiré graphene, *Nature* **595**, 526 (2021).
- [63] J. C. Ward, An identity in quantum electrodynamics, *Phys. Rev.* **78**, 182 (1950).
- [64] Y. Takahashi, On the generalized ward identity, *Il Nuovo Cimento* (1955-1965) **6**, 371 (1957).
- [65] V. Kozii and L. Fu, Odd-parity superconductivity in the vicinity of inversion symmetry breaking in spin-orbit-coupled systems, *Phys. Rev. Lett.* **115**, 207002 (2015).
- [66] S. Sumita and Y. Yanase, Superconductivity induced by fluctuations of momentum-based multipoles, *Phys. Rev. Res.* **2**, 033225 (2020).
- [67] N. E. Bickers, D. J. Scalapino, and S. R. White, Conserving approximations for strongly correlated electron systems: Bethe-salpeter equation and dynamics for the two-dimensional hubbard model, *Phys. Rev. Lett.* **62**, 961 (1989).
- [68] N. Bickers and D. Scalapino, Conserving approximations for strongly fluctuating electron systems. i. formalism and calculational approach, *Annals of Physics* **193**, 206 (1989).
- [69] N. E. Bickers and S. R. White, Conserving approximations for strongly fluctuating electron systems. ii. numerical results and parquet extension, *Phys. Rev. B* **43**, 8044 (1991).
- [70] B. Roulet, J. Gavoret, and P. Nozières, Singularities in the x-ray absorption and emission of metals. i. first-order parquet calculation, *Phys. Rev.* **178**, 1072 (1969).
- [71] N. E. Bickers, Self-consistent many-body theory for condensed matter systems, in *Theoretical Methods for Strongly Correlated Electrons*, edited by D. Sénéchal, A.-M. Tremblay, and C. Bourbonnais (Springer New York, New York, NY, 2004) pp. 237–296.
- [72] Y. Yanase, Random spin-orbit coupling in spin triplet superconductors: Stacking faults in sr2ruo4 and cept3si, *Journal of the Physical Society of Japan* **79**, 084701 (2010).
- [73] M. H. Fischer, F. Loder, and M. Sigrist, Superconductivity and local noncentrosymmetry in crystal lattices, *Phys. Rev. B* **84**, 184533 (2011).
- [74] D. Maruyama, M. Sigrist, and Y. Yanase, Locally non-centrosymmetric superconductivity in multilayer systems, *Journal of the Physical Society of Japan* **81**, 034702 (2012).
- [75] T. Yoshida, M. Sigrist, and Y. Yanase, Pair-density wave states through spin-orbit coupling in multilayer superconductors, *Phys. Rev. B* **86**, 134514 (2012).
- [76] D. Maruyama, M. Sigrist, and Y. Yanase, Spin-orbit coupling in multilayer superconductors with charge imbalance, *Journal of the Physical Society of Japan* **82**, 043703 (2013).
- [77] T. Yoshida, M. Sigrist, and Y. Yanase, Complex-stripe phases induced by staggered rashba spin-orbit coupling, *Journal of the Physical Society of Japan* **82**, 074714 (2013).
- [78] T. Yoshida, M. Sigrist, and Y. Yanase, Parity-mixed superconductivity in locally non-centrosymmetric system, *Journal of the Physical Society of Japan* **83**, 013703 (2014).
- [79] T. Yoshida, M. Sigrist, and Y. Yanase, Topological crystalline superconductivity in locally noncentrosymmetric multilayer superconductors, *Phys. Rev. Lett.* **115**, 027001 (2015).
- [80] T. Hitomi and Y. Yanase, Electric octupole order in bilayer rashba system, *Journal of the Physical Society of Japan* **85**, 124702 (2016), <https://doi.org/10.7566/JPSJ.85.124702>.
- [81] D. Möckli, Y. Yanase, and M. Sigrist, Orbitally limited pair-density-wave phase of multilayer superconductors, *Phys. Rev. B* **97**, 144508 (2018).
- [82] X. Lu and D. Sénéchal, Spin texture in a bilayer high-temperature cuprate superconductor, *Phys. Rev. B* **104**, 024502 (2021).
- [83] A. Skurativska, M. Sigrist, and M. H. Fischer, Spin response and topology of a staggered-rashba superconductor, *Phys. Rev. Res.* **3**, 033133 (2021).
- [84] E. Bauer and M. Sigrist, *Non-centrosymmetric superconductors: introduction and overview*, Vol. 847 (Springer Science & Business Media, 2012).
- [85] See Supplemental Material at [URL will be inserted by publisher].
- [86] H. Watanabe and Y. Yanase, Group-theoretical classification of multipole order: Emergent responses and candidate materials, *Phys. Rev. B* **98**, 245129 (2018).
- [87] S. Hayami, M. Yatsushiro, Y. Yanagi, and H. Kusunose, Classification of atomic-scale multipoles under crystallographic point groups and application to linear response tensors, *Phys. Rev. B* **98**, 165110 (2018).
- [88] M. Yatsushiro, H. Kusunose, and S. Hayami, Multipole classification in 122 magnetic point groups for unified understanding of multiferroic responses and transport phenomena, *Phys. Rev. B* **104**, 054412 (2021).
- [89] Chapter ii - two electrons in a cubic field, in *Multiplets*

- of *Transition-Metal Ions in Crystals*, Pure and Applied Physics, Vol. 33, edited by S. Sugano, Y. Tanabe, and H. Kamimura (Elsevier, 1970) pp. 38–65.
- [90] A. C. Simmonett, I. Pickard, Frank C., I. Schaefer, Henry F., and B. R. Brooks, An efficient algorithm for multipole energies and derivatives based on spherical harmonics and extensions to particle mesh Ewald, *The Journal of Chemical Physics* **140**, 184101 (2014), https://pubs.aip.org/aip/jcp/article-pdf/doi/10.1063/1.4873920/15476588/184101.1_online.pdf.
- [91] M. E. A. Coury, S. L. Dudarev, W. M. C. Foulkes, A. P. Horsfield, P.-W. Ma, and J. S. Spencer, Hubbard-like hamiltonians for interacting electrons in s , p , and d orbitals, *Phys. Rev. B* **93**, 075101 (2016).
- [92] J. Bünemann and F. Gebhard, Coulomb matrix elements in multi-orbital hubbard models, *Journal of Physics: Condensed Matter* **29**, 165601 (2017).
- [93] S. Iimura, M. Hirayama, and S. Hoshino, Multipole representation for anisotropic coulomb interactions, *Phys. Rev. B* **104**, L081108 (2021).
- [94] S. J. Youn, M. H. Fischer, S. H. Rhim, M. Sigrist, and D. F. Agterberg, Role of strong spin-orbit coupling in the superconductivity of the hexagonal pnictide srptas, *Phys. Rev. B* **85**, 220505 (2012).
- [95] J. Goryo, M. H. Fischer, and M. Sigrist, Possible pairing symmetries in srptas with a local lack of inversion center, *Phys. Rev. B* **86**, 100507 (2012).
- [96] J. M. Luttinger and J. C. Ward, Ground-state energy of a many-fermion system. ii, *Phys. Rev.* **118**, 1417 (1960).
- [97] J. M. Luttinger, Fermi surface and some simple equilibrium properties of a system of interacting fermions, *Phys. Rev.* **119**, 1153 (1960).
- [98] G. Baym and L. P. Kadanoff, Conservation laws and correlation functions, *Phys. Rev.* **124**, 287 (1961).
- [99] G. Baym, Self-consistent approximations in many-body systems, *Phys. Rev.* **127**, 1391 (1962).
- [100] H. Yao and F. Yang, Topological odd-parity superconductivity at type-ii two-dimensional van hove singularities, *Phys. Rev. B* **92**, 035132 (2015).
- [101] X. Wu, M. Fink, W. Hanke, R. Thomale, and D. Di Sante, Unconventional superconductivity in a doped quantum spin hall insulator, *Phys. Rev. B* **100**, 041117 (2019).
- [102] K. Nogaki and Y. Yanase, Strongly parity-mixed superconductivity in the rashba-hubbard model, *Phys. Rev. B* **102**, 165114 (2020).
- [103] T. Moriya and K. Ueda, Spin fluctuations and high temperature superconductivity, *Advances in Physics* **49**, 555 (2000).
- [104] Y. Yanase, T. Jujo, T. Nomura, H. Ikeda, T. Hotta, and K. Yamada, Theory of superconductivity in strongly correlated electron systems, *Physics Reports* **387**, 1 (2003).
- [105] M. Houzet and A. Buzdin, Nonuniform superconducting phases in a layered ferromagnetic superconductor, *Europhysics Letters* **58**, 596 (2002).
- [106] A. Buzdin, S. Tollis, and J. Cayssol, Field-induced superconductivity with an enhanced and tunable paramagnetic limit, *Phys. Rev. Lett.* **95**, 167003 (2005).
- [107] S. Tollis, J. Cayssol, and A. Buzdin, Competition between π -coupling and fulde-ferrell-larkin-ovchinnikov modulation in a periodic array of ferromagnetic-superconducting bilayers of atomic thickness, *Phys. Rev. B* **73**, 174519 (2006).
- [108] A. Buzdin, S. Tollis, and J. Cayssol, Anomalous (h,t) phase diagram in bilayered superconducting systems, *Physica C: Superconductivity* **460-462**, 1028 (2007), proceedings of the 8th International Conference on Materials and Mechanisms of Superconductivity and High Temperature Superconductors.
- [109] X. Montiel and A. I. Buzdin, Field-induced superconducting phase in superconductor–normal metal and superconductor-superconductor bilayers, *Phys. Rev. B* **84**, 054518 (2011).
- [110] E. Khalaf, A. J. Kruchkov, G. Tarnopolsky, and A. Vishwanath, Magic angle hierarchy in twisted graphene multilayers, *Phys. Rev. B* **100**, 085109 (2019).
- [111] S. Carr, C. Li, Z. Zhu, E. Kaxiras, S. Sachdev, and A. Kruchkov, Ultraheavy and ultrarelativistic dirac quasiparticles in sandwiched graphenes, *Nano Letters* **20**, 3030 (2020).
- [112] C. Lei, L. Linhart, W. Qin, F. Libisch, and A. H. MacDonald, Mirror symmetry breaking and lateral stacking shifts in twisted trilayer graphene, *Phys. Rev. B* **104**, 035139 (2021).
- [113] S. Onari and H. Kontani, Su(4) Valley + Spin fluctuation interference mechanism for nematic order in magic-angle twisted bilayer graphene: The impact of vertex corrections, *Phys. Rev. Lett.* **128**, 066401 (2022).
- [114] M. Kawamura, Fermisurfer: Fermi-surface viewer providing multiple representation schemes, *Computer Physics Communications* **239**, 197 (2019).

Supplemental Materials:
Field-induced superconductivity mediated by odd-parity multipole fluctuation

S1. SELF-CONSISTENT CONDITION FOR FLUCTUATION EXCHANGE APPROXIMATION

The noninteracting Green functions for $U = 0$ are expressed by the 4×4 matrix form in the spin and sublattice basis,

$$G^{(0)}(\mathbf{k}, i\omega_n) = (i\omega_n s_0 \otimes \sigma_0 - \mathcal{H}(\mathbf{k}))^{-1}, \quad (\text{S1})$$

where $\omega_n = (2n+1)\pi T$ and $\mathcal{H}(\mathbf{k})$ are fermionic Matsubara frequencies and Hamiltonian. Here, s and σ represent spin and sublattice degrees of freedom, respectively. In the interacting case $U \neq 0$, the dressed Green functions contain a self-energy $\Sigma(\mathbf{k}, i\omega_n)$,

$$G(\mathbf{k}, i\omega_n) = (i\omega_n s_0 \otimes \sigma_0 - \mathcal{H}(\mathbf{k}) - \Sigma(\mathbf{k}, i\omega_n))^{-1}. \quad (\text{S2})$$

In the FLEX approximation, the self-energy is expressed with the use of an effective interaction, $\Gamma^n(\mathbf{k}, i\nu_n)$, as

$$\Sigma_{\xi\xi'}(\mathbf{k}, i\omega_n) = \frac{T}{N} \sum_{\mathbf{q}, i\nu_n} \Gamma_{\xi\xi_1\xi'\xi_2}^n(\mathbf{q}, i\nu_n) G_{\xi_1\xi_2}(\mathbf{k} - \mathbf{q}, i\omega_n - i\nu_n), \quad (\text{S3})$$

and the effective interaction is given by

$$\Gamma_{\xi_1\xi_2\xi_3\xi_4}^n(\mathbf{k}, i\nu_n) = U_{\xi_1\xi_2\xi_5\xi_6} \left(\chi_{\xi_5\xi_6\xi_7\xi_8}(\mathbf{k}, i\nu_n) - \frac{1}{2} \chi_{\xi_5\xi_6\xi_7\xi_8}^{(0)}(\mathbf{k}, i\nu_n) \right) U_{\xi_7\xi_8\xi_3\xi_4}, \quad (\text{S4})$$

where $U_{\xi_1\xi_2\xi_3\xi_4}$ is the bare interaction tensor which satisfies the following relation

$$\sum_{\xi_1\xi_2\xi_3\xi_4} U_{\xi_1\xi_2\xi_3\xi_4} c_{\xi_1}^\dagger c_{\xi_2} c_{\xi_3} c_{\xi_4}^\dagger = U \sum_{i,\sigma} n_{i\uparrow\sigma} n_{i\downarrow\sigma}, \quad (\text{S5})$$

$$U_{\xi_1\xi_2\xi_3\xi_4} = \delta_{\sigma_1,\sigma_2} \delta_{\sigma_2,\sigma_3} \delta_{\sigma_3,\sigma_4} U_{s_1 s_2 s_3 s_4}, \quad (\text{S6})$$

$$U_{\uparrow\downarrow\downarrow} = U_{\downarrow\uparrow\uparrow} = -U_{\uparrow\uparrow\downarrow} = -U_{\downarrow\downarrow\uparrow} = U, \quad (\text{S7})$$

and $i\nu_n$ are bosonic Matsubara frequencies. Here, $\chi(\mathbf{k}, i\nu_n)$ is the generalized susceptibility. The abbreviated notation $\xi = (s, \sigma)$ are employed. We introduce the bare susceptibility

$$\chi_{\xi_1\xi_2\xi_3\xi_4}^{(0)}(\mathbf{q}, i\nu_n) = -\frac{T}{N} \sum_{\mathbf{k}, i\omega_n} G_{\xi_1\xi_3}(\mathbf{k}, i\omega_n) G_{\xi_4\xi_2}(\mathbf{k} - \mathbf{q}, i\omega_n - i\nu_n), \quad (\text{S8})$$

and compute the generalized susceptibility by

$$\chi_{\xi_1\xi_2\xi_3\xi_4}(\mathbf{q}, i\nu_n) = \chi_{\xi_1\xi_2\xi_3\xi_4}^{(0)}(\mathbf{q}, i\nu_n) + \chi_{\xi_1\xi_2\xi_5\xi_6}^{(0)}(\mathbf{q}, i\nu_n) U_{\xi_5\xi_6\xi_7\xi_8} \chi_{\xi_7\xi_8\xi_3\xi_4}(\mathbf{q}, i\nu_n). \quad (\text{S9})$$

According to Eqs. (S2)-(S9), G , Σ , Γ^n , $\chi^{(0)}$, and χ depend on each other, and therefore, we self-consistently determine these functions. The FLEX approximation is a conserving approximation in which several conservation laws are satisfied in the framework of the Luttinger-Ward theory [S96–S99].

For functions with fermionic Matsubara frequencies $A(\mathbf{q}, i\omega_n)$, the static limit $A(\mathbf{q}, 0)$ is evaluated by an approximation justified at low temperatures,

$$A(\mathbf{q}, 0) \simeq \frac{A(\mathbf{q}, i\pi T) + A(\mathbf{q}, -i\pi T)}{2}. \quad (\text{S10})$$

For the analysis of superconducting phase transition, particle-particle channel irreducible vertex function Γ^a is needed, and it is obtained by

$$\Gamma_{\xi_1\xi_2\xi_3\xi_4}^a(\mathbf{q}, i\nu_n) = U_{\xi_1\xi_2\xi_3\xi_4}/2 + U_{\xi_1\xi_2\xi_5\xi_6} \chi_{\xi_5\xi_6\xi_7\xi_8}(\mathbf{q}, i\nu_n) U_{\xi_7\xi_8\xi_3\xi_4}. \quad (\text{S11})$$

S2. MULTIPOLE DECOMPOSITION OF SUSCEPTIBILITY

The normalized Pauli matrices ($\bar{\sigma} = \sigma/\sqrt{2}$) and the unit matrix ($\bar{\sigma}^0 = \sigma^0/\sqrt{2}$) compose a complete basis of 2×2 matrix space. Here, we adopt the normalization convention $\text{tr}[(\sigma^\mu)^\dagger \sigma^\mu] = 1$. Namely, any 2×2 complex matrix A can be represented as a linear combination of the normalized Pauli matrices and the unit matrix,

$$A = \sum_{\mu} a_{\mu} \bar{\sigma}^{\mu}, \quad (\text{S12})$$

where a_{μ} are complex coefficients. When A is a Hermitian matrix, a_{μ} should be real numbers. The completeness of the Pauli matrices and the unit matrix leads to the following identity:

$$\sum_{\mu} \bar{\sigma}_{ij}^{\mu} (\bar{\sigma}_{kl}^{\mu})^* = \sum_{\mu} \bar{\sigma}_{ij}^{\mu} \bar{\sigma}_{lk}^{\mu} = \delta_{ik} \delta_{jl}, \quad (\text{S13})$$

where δ_{ij} is Kronecker delta. Here, the Hermite property of the Pauli and unit matrices $\bar{\sigma}_{ij} = (\bar{\sigma}_{ji})^*$ is used in the first equal sign.

The multipole operator in a two-sublattice system is represented by the tensor product of the Pauli matrices in spin- and sublattice-spaces: $\bar{Q}^{\mu\nu} = \bar{s}^{\mu} \otimes \bar{\sigma}^{\nu}$. Consequently, the following identity holds:

$$\sum_{\mathcal{Q}} \bar{Q}_{ij} \bar{Q}_{kl} = \delta_{il} \delta_{jk}. \quad (\text{S14})$$

This identity facilitates the analysis of multipole-resolved fluctuations. It should be noted that extending the current discussion to cases with general N degrees of freedom is straightforward. This involves replacing the Pauli matrix with the $\mathfrak{su}(N)$ Lie algebra.

Upon inserting Eq. (S14), Eq. (S9) can be reformulated into a multipole-resolved form as,

$$\begin{aligned} \chi^{\mathcal{Q}}(\mathbf{q}, i\nu_n) &= \bar{Q}_{\xi_1 \xi_2} \chi_{\xi_2 \xi_1 \xi_3 \xi_4}(\mathbf{q}, i\nu_n) \bar{Q}_{\xi_3 \xi_4} \\ &= \chi^{0, \mathcal{Q}}(\mathbf{q}, i\nu_n) \\ &+ \sum_{\mathcal{Q}' \mathcal{Q}''} \bar{Q}_{\xi_1 \xi_2} \chi_{\xi_2 \xi_1 \xi_5 \xi_6}^0(\mathbf{q}, i\nu_n) \bar{Q}'_{\xi_5 \xi_6} \bar{Q}'_{\xi_7 \xi_8} U_{\xi_8 \xi_7 \xi_9 \xi_{10}} \bar{Q}''_{\xi_9 \xi_{10}} \bar{Q}''_{\xi_{11} \xi_{12}} \chi_{\xi_{12} \xi_{11} \xi_3 \xi_4}(\mathbf{q}, i\nu_n) \bar{Q}_{\xi_3 \xi_4} \end{aligned} \quad (\text{S15})$$

$$\approx \chi^{0, \mathcal{Q}}(\mathbf{q}, i\nu_n) + \chi^{0, \mathcal{Q}}(\mathbf{q}, i\nu_n) U^{\mathcal{Q}} \chi^{\mathcal{Q}}(\mathbf{q}, i\nu_n), \quad (\text{S16})$$

where $U^{\mathcal{Q}} = \bar{Q}_{\xi_1 \xi_2} U_{\xi_1 \xi_2 \xi_3 \xi_4} \bar{Q}_{\xi_4 \xi_3}$. In this final expression, the cross terms between different multipole terms, denoted as $\chi^{\mathcal{Q} \mathcal{Q}'} = \bar{Q}_{\xi_1 \xi_2} \chi_{\xi_1 \xi_2 \xi_3 \xi_4} \bar{Q}'_{\xi_4 \xi_3}$, are ignored. Solving Eq. (S16), we obtain the enhanced multipole susceptibility due to interactions:

$$\chi^{\mathcal{Q}}(q) \approx \frac{\chi^{0, \mathcal{Q}}(q)}{1 - U^{\mathcal{Q}} \chi^{0, \mathcal{Q}}(q)}. \quad (\text{S17})$$

A sufficient condition for achieving a large $\chi^{\mathcal{Q}}(q)$ entails having a large $\chi^{0, \mathcal{Q}}(q)$ and a positive $U^{\mathcal{Q}}$. When we ignore the self-energy, the bare multipole susceptibility $\chi^{0, \mathcal{Q}}(q)$ can be expressed in the band basis as,

$$\begin{aligned} \chi^{0, \mathcal{Q}}(q) &= \bar{Q}_{\beta\alpha} \chi_{\alpha\beta\gamma\delta}^{(0)}(q) \bar{Q}_{\gamma\delta} \\ &= -\bar{Q}_{\beta\alpha} \frac{T}{N} \sum_{\mathbf{k}} G_{\alpha\gamma}(\mathbf{k}) G_{\delta\beta}(\mathbf{k} - \mathbf{q}) \bar{Q}_{\gamma\delta} \\ &= -\bar{Q}_{\beta\alpha} \frac{T}{N} \sum_{\mathbf{k}} U_{\alpha\zeta}(\mathbf{k}) \mathcal{G}_{\zeta}(\mathbf{k}) U_{\gamma\zeta}^*(\mathbf{k}) U_{\delta\eta}(\mathbf{k} - \mathbf{q}) \mathcal{G}_{\eta}(\mathbf{k} - \mathbf{q}) U_{\beta\eta}^*(\mathbf{k} - \mathbf{q}) \bar{Q}_{\gamma\delta} \\ &= -\frac{T}{N} \sum_{\mathbf{k}} (U^\dagger(\mathbf{k} - \mathbf{q}) \bar{Q} U(\mathbf{k}))_{\eta\zeta} \mathcal{G}_{\zeta}(\mathbf{k}) \mathcal{G}_{\eta}(\mathbf{k} - \mathbf{q}) (U^\dagger(\mathbf{k}) \bar{Q} U(\mathbf{k} - \mathbf{q}))_{\zeta\eta} \\ &= -\frac{1}{N} \sum_{\mathbf{k}} \langle u_{\eta, \mathbf{k} - \mathbf{q}} | \bar{Q} | u_{\zeta, \mathbf{k}} \rangle \langle u_{\zeta, \mathbf{k}} | \bar{Q} | u_{\eta, \mathbf{k} - \mathbf{q}} \rangle \times \frac{f(\varepsilon_{\eta}(\mathbf{k} - \mathbf{q})) - f(\varepsilon_{\zeta}(\mathbf{k}))}{i\nu_n + \varepsilon_{\eta}(\mathbf{k} - \mathbf{q}) - \varepsilon_{\zeta}(\mathbf{k})} \\ &= \sum_{\mathbf{k}} \langle u_{\eta, \mathbf{k} - \mathbf{q}} | \bar{Q} | u_{\zeta, \mathbf{k}} \rangle \langle u_{\zeta, \mathbf{k}} | \bar{Q} | u_{\eta, \mathbf{k} - \mathbf{q}} \rangle L_{\zeta\eta}(\mathbf{k}, \mathbf{q}, i\nu_n), \end{aligned} \quad (\text{S18})$$

where $L_{\zeta\eta}(\mathbf{k}, \mathbf{q}, i\nu_n) = -\frac{1}{N}\{f(\varepsilon_\eta(\mathbf{k} - \mathbf{q})) - f(\varepsilon_\zeta(\mathbf{k}))\}/\{i\nu_n + \varepsilon_\eta(\mathbf{k} - \mathbf{q}) - \varepsilon_\zeta(\mathbf{k})\}$ denotes the momentum-resolved Lindhard function between ζ and η bands. Here, $U(\mathbf{k})_{\alpha\zeta} = \langle \alpha | u_{\zeta, \mathbf{k}} \rangle$ represents the unitary matrix that diagonalizes Hamiltonian:

$$U^\dagger(\mathbf{k})\mathcal{H}(\mathbf{k})U(\mathbf{k}) = \mathcal{H}^{\text{diag}}(\mathbf{k}), \quad (\text{S19})$$

$$\mathcal{H}(\mathbf{k}) |u_{\zeta, \mathbf{k}}\rangle = \varepsilon_\zeta(\mathbf{k}) |u_{\zeta, \mathbf{k}}\rangle. \quad (\text{S20})$$

The Green function in the band basis is given by

$$\begin{aligned} \mathcal{G}(k) &= U^\dagger(\mathbf{k})G(k)U(\mathbf{k}), \\ \mathcal{G}_\zeta(k) &= \frac{1}{i\omega_n - \varepsilon_\zeta(\mathbf{k})}. \end{aligned} \quad (\text{S21})$$

In the same manner, we can decompose the effective interaction $\Gamma^n(q)$ [as defined in Eq. (S4)] and $\Gamma^a(q)$ [as defined in Eq. (S11)] into their respective multipole channels. The decomposition is expressed as follows:

$$\Gamma^{n, \mathcal{Q}}(q) \approx U^\mathcal{Q} \left(\chi^\mathcal{Q}(q) - \frac{1}{2}\chi^{0, \mathcal{Q}}(q) \right) U^\mathcal{Q}, \quad (\text{S22})$$

$$\Gamma^{a, \mathcal{Q}}(q) \approx \frac{U^\mathcal{Q}}{2} + U^\mathcal{Q}\chi^\mathcal{Q}(q)U^\mathcal{Q}. \quad (\text{S23})$$

In Eq. (S22), the effective interaction for the particle-hole channel, $\Gamma^{n, \mathcal{Q}}(q)$, is expressed as a function of the multipole susceptibility $\chi^\mathcal{Q}(q)$ and the bare susceptibility $\chi^{0, \mathcal{Q}}(q)$ modulated by the interaction $U^\mathcal{Q}$. Similarly, Eq. (S23) depicts the effective interaction for the particle-particle channel, $\Gamma^{a, \mathcal{Q}}(q)$, also as a function of the multipole susceptibility and interaction.

S3. COOPER PAIRING CHANNEL FROM MULTIPOLE FLUCTUATIONS

In this section, we give a comprehensive classification of Cooper pairing channels mediated by multipole fluctuations. First, we summarize Cooper pairing channel decomposition in the presence of a single degree of freedom σ ,

$$S^{\sigma_0} = \bar{\psi}_\alpha \sigma_{\alpha\beta}^0 \psi_\beta V^{\sigma_0} \bar{\psi}_\gamma \sigma_{\gamma\delta}^0 \psi_\delta = \frac{1}{2} V^{\sigma_0} \left\{ \hat{p}^{0, \dagger} \hat{p}^0 + \hat{p}^{x, \dagger} \hat{p}^x + \hat{p}^{y, \dagger} \hat{p}^y + \hat{p}^{z, \dagger} \hat{p}^z \right\}, \quad (\text{S24})$$

$$S^{\sigma_x} = \bar{\psi}_\alpha \sigma_{\alpha\beta}^x \psi_\beta V^{\sigma_x} \bar{\psi}_\gamma \sigma_{\gamma\delta}^x \psi_\delta = \frac{1}{2} V^{\sigma_x} \left\{ \hat{p}^{0, \dagger} \hat{p}^0 + \hat{p}^{x, \dagger} \hat{p}^x - \hat{p}^{y, \dagger} \hat{p}^y - \hat{p}^{z, \dagger} \hat{p}^z \right\}, \quad (\text{S25})$$

$$S^{\sigma_y} = \bar{\psi}_\alpha \sigma_{\alpha\beta}^y \psi_\beta V^{\sigma_y} \bar{\psi}_\gamma \sigma_{\gamma\delta}^y \psi_\delta = \frac{1}{2} V^{\sigma_y} \left\{ -\hat{p}^{0, \dagger} \hat{p}^0 + \hat{p}^{x, \dagger} \hat{p}^x - \hat{p}^{y, \dagger} \hat{p}^y + \hat{p}^{z, \dagger} \hat{p}^z \right\}, \quad (\text{S26})$$

$$S^{\sigma_z} = \bar{\psi}_\alpha \sigma_{\alpha\beta}^z \psi_\beta V^{\sigma_z} \bar{\psi}_\gamma \sigma_{\gamma\delta}^z \psi_\delta = \frac{1}{2} V^{\sigma_z} \left\{ \hat{p}^{0, \dagger} \hat{p}^0 - \hat{p}^{x, \dagger} \hat{p}^x - \hat{p}^{y, \dagger} \hat{p}^y + \hat{p}^{z, \dagger} \hat{p}^z \right\}, \quad (\text{S27})$$

where the Cooper pair operators are defined by $\hat{P}^\mu = \psi_\alpha \sigma_{\alpha\beta}^\mu \psi_\beta$. Here, the following identities on the Pauli and unit matrix are used [S66].

$$\sigma_{\alpha\beta}^0 \sigma_{\gamma\delta}^0 = \frac{1}{2} \left(\sigma_{\alpha\gamma}^0 \sigma_{\delta\beta}^0 + \sigma_{\alpha\gamma}^x \sigma_{\delta\beta}^x + \sigma_{\alpha\gamma}^y \sigma_{\delta\beta}^y + \sigma_{\alpha\gamma}^z \sigma_{\delta\beta}^z \right), \quad (\text{S28})$$

$$\sigma_{\alpha\beta}^x \sigma_{\gamma\delta}^x = \frac{1}{2} \left(\sigma_{\alpha\gamma}^0 \sigma_{\delta\beta}^0 + \sigma_{\alpha\gamma}^x \sigma_{\delta\beta}^x - \sigma_{\alpha\gamma}^y \sigma_{\delta\beta}^y - \sigma_{\alpha\gamma}^z \sigma_{\delta\beta}^z \right), \quad (\text{S29})$$

$$\sigma_{\alpha\beta}^y \sigma_{\gamma\delta}^y = \frac{1}{2} \left(-\sigma_{\alpha\gamma}^0 \sigma_{\delta\beta}^0 + \sigma_{\alpha\gamma}^x \sigma_{\delta\beta}^x - \sigma_{\alpha\gamma}^y \sigma_{\delta\beta}^y + \sigma_{\alpha\gamma}^z \sigma_{\delta\beta}^z \right), \quad (\text{S30})$$

$$\sigma_{\alpha\beta}^z \sigma_{\gamma\delta}^z = \frac{1}{2} \left(\sigma_{\alpha\gamma}^0 \sigma_{\delta\beta}^0 - \sigma_{\alpha\gamma}^x \sigma_{\delta\beta}^x - \sigma_{\alpha\gamma}^y \sigma_{\delta\beta}^y + \sigma_{\alpha\gamma}^z \sigma_{\delta\beta}^z \right). \quad (\text{S31})$$

Next, for the multipole composed of spin and sublattice degrees of freedom as in the case of our model, we obtain the Cooper pairing channel as follows:

$$S^\mathcal{Q} = \bar{\psi}_\alpha \mathcal{Q}_{\alpha\beta}^{\mu\nu} \psi_\beta V^\mathcal{Q} \bar{\psi}_\gamma \mathcal{Q}_{\gamma\delta}^{\mu\nu} \psi_\delta \quad (\text{S32})$$

$$= \bar{\psi}_{s_\alpha \sigma_\alpha} \bar{s}_{s_\alpha s_\beta}^\mu \bar{\sigma}_{\sigma_\alpha \sigma_\beta}^\nu \psi_{s_\beta \sigma_\beta} V^\mathcal{Q} \bar{\psi}_{s_\gamma \sigma_\gamma} \bar{s}_{s_\gamma s_\delta}^\mu \bar{\sigma}_{\sigma_\gamma \sigma_\delta}^\nu \psi_{s_\delta \sigma_\delta} \quad (\text{S33})$$

$$= V^\mathcal{Q} \bar{\psi}_{s_\alpha \sigma_\alpha} \bar{\psi}_{s_\gamma \sigma_\gamma} \psi_{s_\delta \sigma_\delta} \psi_{s_\beta \sigma_\beta} \bar{s}_{s_\alpha s_\beta}^\mu \bar{s}_{s_\gamma s_\delta}^\mu \bar{\sigma}_{\sigma_\alpha \sigma_\beta}^\nu \bar{\sigma}_{\sigma_\gamma \sigma_\delta}^\nu. \quad (\text{S34})$$

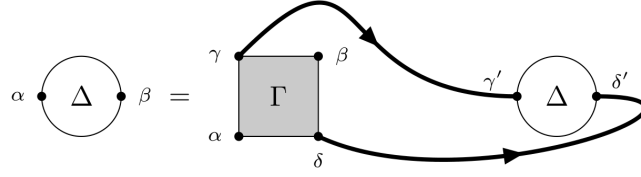


FIG. S1. The diagrammatic representation of the Éliashberg equation. The shaded square and the black line represent the irreducible four-point vertex function in the particle-particle channel and the single-particle Green function, respectively.

For example, if we take $\mu = x$ and $\nu = y$, Cooper pairing channel is given as follows:

$$\mathcal{S}^{\mathcal{Q}^{xy}} = \frac{V^{\mathcal{Q}}}{4} \left\{ -\hat{p}^{00,\dagger}\hat{p}^{00} + \hat{p}^{0x,\dagger}\hat{p}^{0x} - \hat{p}^{0y,\dagger}\hat{p}^{0y} + \hat{p}^{0z,\dagger}\hat{p}^{0z} - \hat{p}^{x0,\dagger}\hat{p}^{x0} + \hat{p}^{xx,\dagger}\hat{p}^{xx} - \hat{p}^{xy,\dagger}\hat{p}^{xy} + \hat{p}^{xz,\dagger}\hat{p}^{xz} \right. \\ \left. + \hat{p}^{y0,\dagger}\hat{p}^{y0} - \hat{p}^{yx,\dagger}\hat{p}^{yx} + \hat{p}^{yy,\dagger}\hat{p}^{yy} - \hat{p}^{yz,\dagger}\hat{p}^{yz} + \hat{p}^{z0,\dagger}\hat{p}^{z0} - \hat{p}^{zx,\dagger}\hat{p}^{zx} + \hat{p}^{zy,\dagger}\hat{p}^{zy} - \hat{p}^{zz,\dagger}\hat{p}^{zz} \right\}. \quad (\text{S35})$$

Other decomposed Cooper pairing channels are summarized in Appendix. A.

S4. ÉLIASHBERG EQUATION

To investigate superconductivity, we adopt the linearized Éliashberg equation which is expressed as

$$\lambda \Delta_{\alpha\beta}(k) = \frac{T}{N} \sum_{k'} \Gamma_{\alpha\gamma\delta\beta}^a(k-k') G_{\gamma\gamma'}(k) \Delta_{\gamma'\delta'}(k) G_{\delta\delta'}(-k), \quad (\text{S36})$$

where Δ is the gap function and Γ^a is the particle-particle channel irreducible vertex function obtained in Eq. (S11). Figure S1 shows the diagrammatic representation of the linearized Éliashberg equation. With the power method, we numerically evaluate λ , eigenvalues of the linearized Éliashberg equation, and determine the critical temperature T_c from the criterion $\lambda = 1$.

S5. DIAGRAMMATIC CONSIDERATION ON THE STABILITY OF ODD-PARITY SUPERCONDUCTING PHASE

This section elucidates the distinctive role of inter-sublattice pairing in the field-induced odd-parity superconductivity. Utilizing the diagrammatic expression of the Éliashberg equation, we specify the important scattering process. While simplification is attained by solely considering the transverse spin fluctuation denoted by χ^{\pm} or χ^{\mp} , expanding the following analysis to include longitudinal spin fluctuation χ^{zz} is straightforward. In the following, we denote the dominant intra-sublattice spin-singlet component in the A and B sublattices as $\psi^{\text{AA}}(\mathbf{k})$ and $\psi^{\text{BB}}(\mathbf{k})$, respectively.

The scattering processes illustrated in Figs. S2(a-b) highlight how the unusual inter-sublattice pairing, represented by $\Im d_z^{\text{AB}}(\mathbf{k}) s_z i s_y \otimes \sigma_y$, introduces the attractive force between $\psi^{\text{AA}}(\mathbf{k})$ and $\psi^{\text{BB}}(\mathbf{k})$. By amalgamating these two diagrams and tracing out the gap function d_z^{BA} , a composite diagram elucidating the second-order scattering process between $\psi^{\text{AA}}(\mathbf{k})$ and $\psi^{\text{BB}}(\mathbf{k})$ is derived. Due to the positive sign of χ_{AA}^{\pm} and the negative sign of χ_{BA}^{\mp} [see Fig. S2(c,d)], the overall sign of this second-order scattering process is negative. This scattering process with negative sign necessitates a sign change of gap functions through $2\mathbf{q} = (0, 0)$ momentum transfer, a condition intrinsically met due to the relation $\psi^{\text{AA}}(\mathbf{k}) = -\psi^{\text{BB}}(\mathbf{k})$. Notably, spin-orbit coupling is not required in this mechanism, thereby implying that field-induced superconductivity can be achieved in materials with weak spin-orbit coupling.

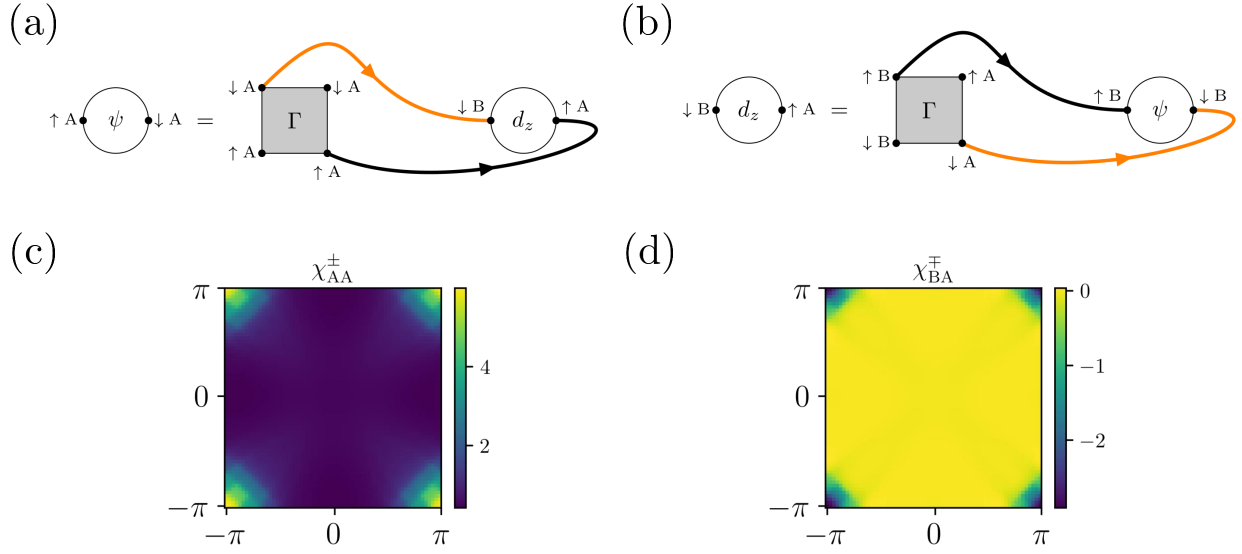


FIG. S2. (a) (b) The diagrammatic representation of the dominant scattering process between the Cooper pairs represented by ψ^{AA} , ψ^{BB} , and d_z^{AB} . The black line and orange line represent the intra-sublattice Green function $G^{AA}(k)$ and the inter-sublattice Green function $G^{AB}(k)$, respectively. The scattering process between d_z^{AB} and ψ^{AA} or ψ^{BB} via the transverse magnetic fluctuation are shown. (c) The momentum dependence of the intra-sublattice transverse magnetic fluctuation which appears in the diagram (a). (d) The momentum dependence of the inter-sublattice transverse magnetic fluctuation which appears in the diagram (b).

